HHS Public Access

Author manuscript

RSC Adv. Author manuscript; available in PMC 2017 October 26.

Published in final edited form as:

RSC Adv. 2016 ; 6(105): 103618–103621. doi:10.1039/C6RA20439B.

Copper (II)-doped semiconducting polymer dots for nitroxyl imaging in live cells

Xu Wu[a], **Li Wu**[a], **I-Che Wu**[a], and **Daniel T. Chiu**[a,*]

[a]Department of Chemistry and Bioengineering, University of Washington, Seattle, WA, USA

Abstract

The first nanoparticle-based fluorescent probe for the specific detection of nitroxyl (HNO) was designed and constructed by doping copper(II) into semiconducting polymer dots (Pdots). The probe turns on and fluoresces in the presence of HNO. We used the new sensor to monitor changes of HNO levels in live cells.

Nitroxyl (HNO), one of the reactive nitrogen species (RNS), plays important roles in various physiological and pathological pathways.[1, 2] For example, HNO is recognized as a promising drug for the treatment of heart failure and some cancers as well as in the mitigation of ischemia-reperfusion injury and alcoholism.[3-5] The enzyme aldehyde dehydrogenase might be inhibited by HNO through its reaction with thiol groups.[6] Therefore, the development of probes with high sensitivity and selectivity for HNO detection in biological systems will find use in these applications.

Traditional analytical methods, such as colorimetric method, HPLC, mass spectrometry, and electrochemical analysis, were developed for HNO detection.[7-10] However, these methods are ineffective for *in situ* monitoring of HNO in biological samples. Recently, several fluorescence assays for HNO detection have been developed due to their high sensitivity, high spatiotemporal resolution, and real-time imaging ability in biological systems, including cells and tissues.[11-16]

The reported fluorescence assays for HNO detection fall into two main categories, metal-based[11, 15, 17] and phosphine-based molecular probes.[13, 18-20] However, these probes can be sensitive to fluctuations of the biological conditions, such as pH.[18, 19] Another limitation of these probes is that most of them are not water-soluble. Small portions of organic solvents, such as DMSO and ethanol, are required to dissolve these probes for biological imaging.[12, 21, 22] Development of these nitroxyl probes also require expertise in chemical design and synthesis. To address these issues of probes based on fluorescent molecules, fluorescent nanoparticles are good candidates. They are simple to design and develop, bright for fluorescence imaging, water-soluble, and relatively inexpensive.[23-25]

* chiu@uw.edu; Fax: +1 206-685-8665. .

Electronic Supplemantary Information (ESI) available: [details of any supplementary information available should be included here]. See DOI: 10.1039/x0xx00000x

‡Footnotes relating to the main text should appear here. These might include comments relevant to but not central to the matter under discussion, limited experimental and spectral data, and crystallographic data.

Recently, semiconducting polymer dots (Pdots) were developed as fluorescent probes with high brightness, good photostability, water solubility, and low toxicity for both small-molecule sensing and biological imaging.[26-30] We recently fabricated a serious of Pdots with excellent photophysical properties and applied them to the field of biological sensing and biological imaging.[31-36] In this communication, we developed a strategy for quantitative detection of HNO using copper (II)-doped PFBT polymer dot (Pdot-PFBT/PC_{30}-Cu^{2+}). Scheme 1 describes the fabrication of Pdot-PFBT/PC_{30}-Cu^{2+}. The Pdots were doped with Cu^{2+} ions by chelating with the carboxyl groups on the carboxylic acid-functionalized PFBT polymers (PC_{30}). The fluorescence of Pdots was quenched by the Cu^{2+} through electron transfer. As reported in the literature, HNO can selectively reduce Cu^{2+} to Cu^{+}. The reduction by HNO can lead to the disruption of the electron transfer process and thus turn on fluorescence from the Pdots.[11, 37, 38]

In our design, we anticipate two advantages over the previous probes for HNO. The first is that the Cu^{2+} is doped in the Pdots, which will decrease the interference by other species, especially biological reductants. The second advantage is the water solubility, high photostability, biocompatibility and high brightness of Pdots, which facilitate the sensitive detection and imaging of HNO in live cells.

The size and morphology of the Pdots-PFBT/PC_{30}-Cu^{2+} were characterized by transmission electron microscopy (TEM, Fig. 1a) and dynamic light scattering (DLS, Fig. 1b). The Pdot-PFBT/PC_{30}-Cu^{2+} showed a hydrodynamic diameter of 32.1 ± 1.6 nm, which is consistent with the TEM images (31.6 ± 6.7 nm). The doping of Cu^{2+} into Pdots not only quenched the fluorescence, but also affected the size of Pdots. Thus, we optimized the amount of Cu^{2+} doped into Pdots during preparation to achieve high quenching efficiency of the Pdot fluorescence while maintaining a small Pdot size. As shown in Fig. S1, 0.22 mg of $CuCl_2$ with 0.25 mg PC_{30} resulted in Pdots with relative small size while offering good quenching efficiency of the Pdots.

The photophysical properties of Pdot-PFBT/PC_{30} and Pdot-PFBT/PC_{30}-Cu^{2+} in 10 mM PBS solution (pH = 7.4) are summarized in Table S1 in the supplementary information. As shown in Fig. 2a, after the addition of Cu^{2+}, the absorbance peak of the Pdots at 350 nm increased while their absorbance at 450 nm decreased; this might be caused by the interaction between Cu^{2+} and the PFBT polymer in the Pdots. This finding is in contrast to our previous report,[33] where we found that adding Cu^{2+} into the formed Pdots did not cause the absorption change because Cu^{2+} only induced the Pdots to aggregate. In that previous report, the fluorescence was quenched by aggregation. The absorption spectra change in this case suggests that the quenching of fluorescence was induced by the electron transfer between polymer and Cu^{2+}. Therefore, the difference between this work and our previous report lies mainly in how Cu^{2+} was introduced. Rather than sensing Cu^{2+} using already formed Pdots that we reported, here Cu^{2+} was doped inside the Pdot as it was formed, thus in close proximity to the polymer to quench Pdot fluorescence. The fluorescence intensity decreased about 71% when Cu^{2+} was added into the Pdot-PFBT/PC_{30} (Fig. 2b), which is consistent with the results of the quantum yield measurements. The quantum yield of Pdot-PFBT/PC_{30} decreased from 15.5 % to 3.8 % in Pdot-PFBT/PC_{30}-Cu^{2+} because of the quenching by Cu^{2+}.

After we found that the Cu^{2+} doped in Pdots significantly quenched the fluorescence of Pdots, we first investigated the optical response of Pdot-PFBT/PC_{30}-Cu^{2+} to Angeli's salt (AS), which is a source for HNO in PBS buffer (10 mM, pH 7.4). As shown in Fig. 2b, the fluorescence intensity of Pdot-PFBT/PC_{30}-Cu^{2+} exhibited approximately a doubling of the fluorescence enhancement after 20 min with the addition of 800 μM AS in PBS solution.

Next, we studied the kinetic properties of Pdot-PFBT/PC_{30}-Cu^{2+} by adding AS in the PBS solution. The fluorescence intensity at 537 nm was monitored over time after adding AS in PBS buffer. As shown in Fig. 2c, Pdot-PFBT/PC_{30}-Cu^{2+} exhibited a quick response to AS (400 μM) and reached plateau around 15 min. We therefore chose 20 min as the end point for the subsequent experiments. Compared to the addition of AS, NaOH introduction did not change the fluorescence intensity (Fig. 2c), and thus this probe is not sensitive to physiological variations in pH.

In order to use the probes for imaging HNO in cells, their photostability is an important parameter. We tested the photostability of Pdot-PFBT/PC_{30}-Cu^{2+}. As shown in Fig. 2d, the fluorescence intensity of Pdot-PFBT/PC_{30}-Cu^{2+} barely changed after illumination over 1 hour. In contrast, quantum dots (QDs-525) decreased about 10 % under the same experimental condition, indicating the good photostability of Pdot-PFBT/PC_{30}-Cu^{2+}. We also investigated the effect of pH on the fluorescence of Pdot-PFBT/PC_{30}-Cu^{2+}. The results (Fig. S2) showed that Pdot-PFBT/PC_{30}-Cu^{2+} were stable within a pH range from 4.5 to 10.5. Thus, Pdot-PFBT/PC_{30}-Cu^{2+} can detect HNO without being affected by photobleaching and pH fluctuation under physiological conditions.

A detailed titration experiment of the Pdot-PFBT/PC_{30}-Cu^{2+} with AS was performed to determine the detection limit of the method. When 1 ppm of Pdots-PFBT/PC_{30}-Cu^{2+} was treated with various concentrations of AS (from 0 μM to 800 μM), the fluorescence intensity at 537 nm was gradually enhanced (Fig. 3a and b). This indicated that the quenching of Pdots by Cu^{2+} was restored after the reduction by HNO to Cu^{+}. The fluorescence enhancement of Pdots-PFBT/PC_{30}-Cu^{2+} was plotted against the AS concentration. It showed a linear relationship to the concentration in the range of 10-100 μM (Fig. 3c). The calibration curve showed a regression equation of $F/F_0 = 0.005\ [AS] + 1.103$ with $R^2 = 0.974$. The detection limit was determined to be 6 μM based on the 3σ/slope method, which is comparable to or better than several reported copper-based fluorophore probes with limit of detection in the range of 50 – 100 μM.[15, 37]

We then evaluated the detection specificity of Pdot-PFBT/PC_{30}-Cu^{2+} for HNO over other reactive species in PBS solution. As shown in Fig. 4, no significant changes in emission were observed in the presence of high concentrations of biological oxidants (Fe^{3+}, H_2O_2, NO_2^-, NO_3^-, and ClO^-), biological reductants (ascorbic acid (AA), cysteine (Cys) and glutathione (GSH)), and several other cationic and anionic ions (K^+, Zn^{2+}, Mg^{2+}, F^-, N_3^- and O_2^-). The interference of the biological reductants during HNO detection always is a roadblock for Cu^{2+}-based probes.[14] We believe the Pdot-based probes were insensitive to reductants because these biological reductants had limited access to the doped Cu^{2+} in Pdots. However, this observation needs further investigation. In contrast, introduction of AS

(800 μM) induced a large fluorescence enhancement. These results indicated that the Pdot-PFBT/PC_{30}-Cu^{2+} are selective for HNO over other tested redox species.

Encouraged by the promising properties of Pdot-PFBT/PC_{30}-Cu^{2+}, we next studied their HNO imaging capabilities within live cells. The cell cytotoxicity of Pdot-PFBT/PC_{30}-Cu^{2+} was first investigated by the methylthiazolyltetrazolium (MTT) assay. As shown in Fig. S3, 1 – 20 ppm of Pdot-PFBT/PC_{30}-Cu^{2+} were incubated with MCF-7 cells (American Type Culture Collection (ATCC, Manassas, VA, USA) for 24 hours. Cytotoxicity was negligible until the concentration of Pdots reached 10 ppm. The results demonstrated the good biocompatibility of the Pdots. In the HNO imaging studies, MCF-7 cells were first incubated with 5 ppm of Pdot-PFBT/PC_{30}-Cu^{2+} for 24 hours in a glass-bottomed culture dish at 37 °C. The cells were then incubated with and without AS for another 20 min at 37 °C, after which the fluorescence images were taken. As shown in Fig. 5, the cells without treatment of AS displayed weak green fluorescence. In contrast, in the presence of 1 mM AS, the MCF-7 cells emitted strong green fluorescence. As shown in Fig. 4, most of the reactive species in cells do not appear to interfere with the detection of HNO using Pdot-PFBT/PC_{30}-Cu^{2+}, most likely because Cu^{2+} is protected from these interfering species if they cannot diffuse into the Pdot to reach the Cu^{2+} The quantitative monitoring of HNO levels in cells can be carried out by calculating the fluorescence enhancement of the Pdot and quantify it using the calibration curve in Fig 3. The fluorescence enhancement with AS treatment clearly demonstrated that Pdot-PFBT/PC_{30}-Cu^{2+} can be used for HNO imaging in live cells.

Conclusions

In summary, we have constructed the first nanoparticle-based fluorescent HNO probe using copper (II)-doped Pdots. The Pdot-PFBT/PC_{30}-Cu^{2+} exhibit high sensitivity and selectivity for HNO detection. As we demonstrated with our imaging experiments, the Pdot-PFBT/PC_{30}-Cu^{2+} was able to monitor the changes of HNO levels in live cells. Compared with the present molecular fluorescent probes for HNO detection, Pdot-PFBT/PC_{30}-Cu^{2+} possesses several advantages: (i) No complex molecular design and organic synthesis were required to construct the Pdots; (ii) No organic solvent was necessary to dissolve the probes because the Pdots were highly soluble in water; (iii) Excellent photostability and no pH response of Pdots ensured the long-term imaging and minimum effect of physiological fluctuation. We finally note that the surface of Pdots are decorated with carboxyl groups, which are amenable to bioconjugation with specific tags that allow the Pdots to be used for targeted labelling and imaging.[39, 40]

Supplementary Material

Refer to Web version on PubMed Central for supplementary material.

Acknowledgements

We gratefully acknowledge support of this work by the National Institutes of Health (CA186798) and by the Solid Tumor Translational Research, Fred Hutchinson Cancer Research Center.

references

1. Xu W, Liu LZ, Loizidou M, Ahmed M, Charles IG. Cell Res. 2002; 12:311–320. [PubMed: 12528889]
2. Münzel T, Feil R, Mülsch A, Lohmann SM, Hofmann F, Walter U. Circulation. 2003; 108:2172–2183. [PubMed: 14597579]
3. Paolocci N, Katori T, Champion HC, St John ME, Miranda KM, Fukuto JM, Wink DA, Kass DA. Proc. Natl. Acad. Sci. U.S.A. 2003; 100:5537–5542. [PubMed: 12704230]
4. Sherman MP, Grither WR, McCulla RD. J. Org. Chem. 2010; 75:4014–4024. [PubMed: 20481507]
5. Paolocci N, Saavedra WF, Miranda KM, Martignani C, Isoda T, Hare JM, Espey MG, Fukuto JM, Feelisch M, Wink DA, Kass DA. Proc. Natl. Acad. Sci. U.S.A. 2001; 98:10463–10468. [PubMed: 11517312]
6. DeMaster EG, Redfern B, Nagasawa HT. Biochem Pharmacol. 1998; 55:2007–2015. [PubMed: 9714321]
7. Cline MR, Tu C, Silverman DN, Toscano JP. Free Radic. Biol. Med. 2011; 50:1274–1279. [PubMed: 21349325]
8. Bari SE, Martí MA, Amorebieta VT, Estrin DA, Doctorovich F. J. Am. Chem. Soc. 2003; 125:15272–15273. [PubMed: 14664554]
9. Suarez SA, Bikiel DE, Wetzler DE, Marti MA, Doctorovich F. Anal. Chem. 2013; 85:10262–10269. [PubMed: 23952708]
10. Reisz JA, Klorig EB, Wright MW, King SB. Org. Lett. 2009; 11:2719–2721. [PubMed: 19492805]
11. Rivera-Fuentes P, Lippard SJ. Acc. Chem. Res. 2015; 48:2927–2934. [PubMed: 26550842]
12. Zhang H, Liu R, Tan Y, Xie WH, Lei H, Cheung HY, Sun H. ACS Appl. Mater. Interfaces. 2015; 7:5438–5443. [PubMed: 25658137]
13. Kawai K, Ieda N, Aizawa K, Suzuki T, Miyata N, Nakagawa H. J. Am. Chem. Soc. 2013; 135:12690–12696. [PubMed: 23865676]
14. Kim S, Minier MA, Loas A, Becker S, Wang F, Lippard SJ. J. Am. Chem. Soc. 2016; 138:1804–1807. [PubMed: 26836121]
15. Wrobel AT, Johnstone TC, Deliz Liang A, Lippard SJ, Rivera-Fuentes P. J. Am. Chem. Soc. 2014; 136:4697–4705. [PubMed: 24564324]
16. Dong B, Zheng K, Tang Y, Lin W. J. Mater. Chem. B. 2016; 4:1263–1269.
17. Royzen M, Wilson JJ, Lippard SJ. J. Inorg. Biochem. 2013; 118:162–170. [PubMed: 23102502]
18. Liu C, Wu H, Wang Z, Shao C, Zhu B, Zhang X. Chem. Commun. 2014; 50:6013–6016.
19. Mao GJ, Zhang XB, Shi XL, Liu HW, Wu YX, Zhou LY, Tan W, Yu RQ. Chem. Commun. 2014; 50:5790–5792.
20. Zheng K, Lin W, Cheng D, Chen H, Liu Y, Liu K. Chem. Commun. 2015; 51:5754–5757.
21. Jing X, Yu F, Chen L. Chem. Commun. 2014; 50:14253–14256.
22. Apfel UP, Buccella D, Wilson JJ, Lippard SJ. Inorg. Chem. 2013; 52:3285–3294. [PubMed: 23461436]
23. Bogart LK, Pourroy G, Murphy CJ, Puntes V, Pellegrino T, Rosenblum D, Peer D, Lévy R. ACS Nano. 2014; 8:3107–3122. [PubMed: 24641589]
24. Li J, Cheng F, Huang H, Li L, Zhu JJ. Chem. Soc. Rev. 2015; 44:7855–7880. [PubMed: 26214317]
25. Yao J, Yang M, Duan Y. Chem. Rev. 2014; 114:6130–6178. [PubMed: 24779710]
26. Wu C, Chiu DT. Angew. Chem. Int. Ed. 2013; 52:3086–3109.
27. Pu K, Shuhendler AJ, Rao J. Angew. Chem. Int. Ed. 2013; 52:10325–10329.
28. Shuhendler AJ, Pu K, Cui L, Uetrecht JP, Rao J. Nat. Biotechnol. 2014; 32:373–380. [PubMed: 24658645]
29. Hong G, Zou Y, Antaris AL, Diao S, Wu D, Cheng K, Zhang X, Chen C, Liu B, He Y, Wu JZ, Yuan J, Zhang B, Tao Z, Fukunaga C, Dai H. Nat. Commun. 2014; 5:4206. [PubMed: 24947309]
30. Xiong L, Shuhendler AJ, Rao J. Nat. Commun. 2012; 3:1193. [PubMed: 23149738]
31. Chan YH, Wu C, Ye F, Jin Y, Smith PB, Chiu DT. Anal. Chem. 2011; 83:1448–1455. [PubMed: 21244093]

32. Ye F, Wu C, Jin Y, Chan YH, Zhang X, Chiu DT. J. Am. Chem. Soc. 2011; 133:8146–8149. [PubMed: 21548583]
33. Chan YH, Jin Y, Wu C, Chiu DT. Chem. Commun. 2011; 47:2820–2822.
34. Chan YH, Ye F, Gallina ME, Zhang X, Jin Y, Wu IC, Chiu DT. J. Am. Chem. Soc. 2012; 134:7309–7312. [PubMed: 22515545]
35. Wu I, Yu J, Ye F, Rong Y, Gallina ME, Fujimoto BS, Zhang Y, Chan Y, Sun W, Zhou X, Wu C, Chiu DT. J. Am. Chem. Soc. 2015; 137:173–178. [PubMed: 25494172]
36. Sun K, Tang Y, Li Q, Yin S, Qin W, Yu J, Chiu DT, Liu Y, Yuan Z, Zhang X, Wu C. ACS Nano. 2016; 10:6769–6781. [PubMed: 27303785]
37. Rosenthal J, Lippard SJ. J. Am. Chem. Soc. 2010; 132:5536–5537. [PubMed: 20355724]
38. Zhou Y, Liu K, Li JY, Fang Y, Zhao TC, Yao C. Org. Lett. 2011; 13:1290–1293. [PubMed: 21322578]
39. Zhang Y, Ye F, Sun W, Yu J, Wu IC, Rong Y, Zhang Y, Chiu DT. Chem. Sci. 2015; 6:2102–2109. [PubMed: 25709806]
40. Rong Y, Yu J, Zhang X, Sun W, Ye F, Wu IC, Zhang Y, Hayden S, Zhang Y, Wu C, Chiu DT. ACS Macro. Lett. 2014; 3:1051–1054. [PubMed: 25419486]

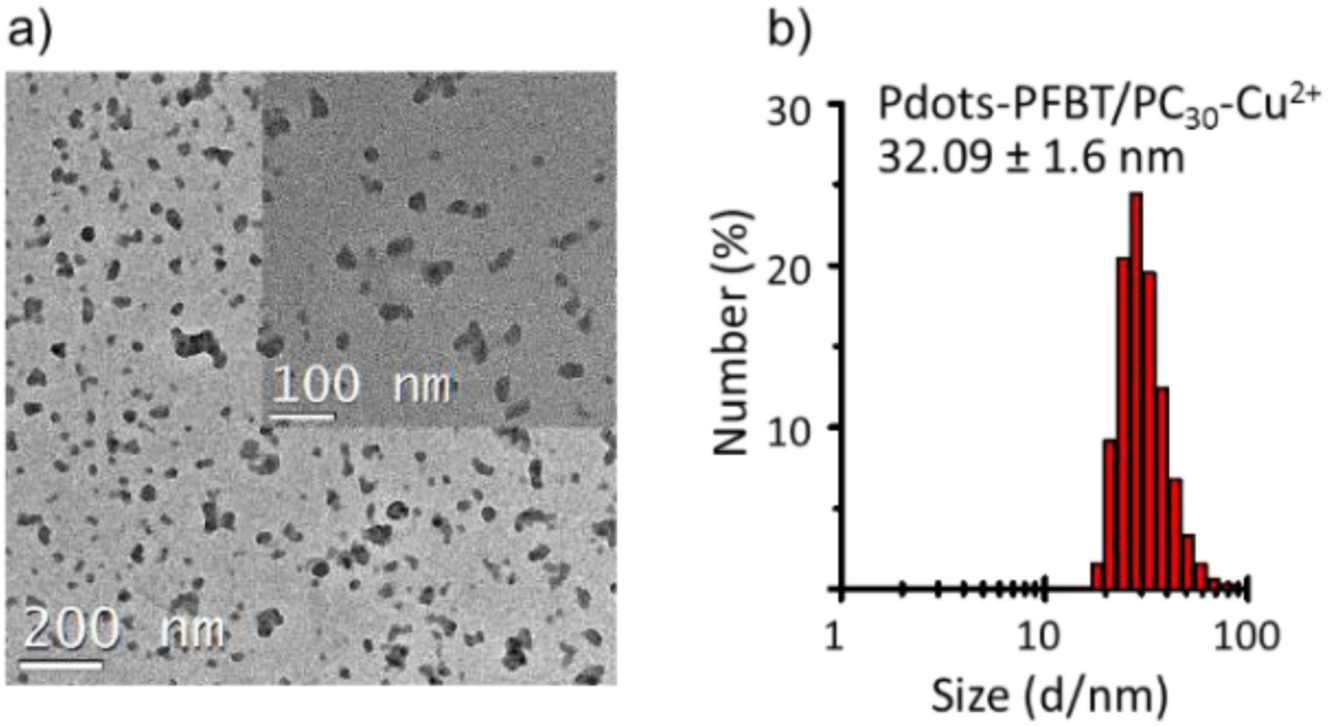

Fig. 1.

TEM image (a) and hydrodynamic diameter measured by DLS (b) of Pdot-PFBT/PC_{30}-Cu^{2+}. The scale bar of inset of (a) is 50 nm.

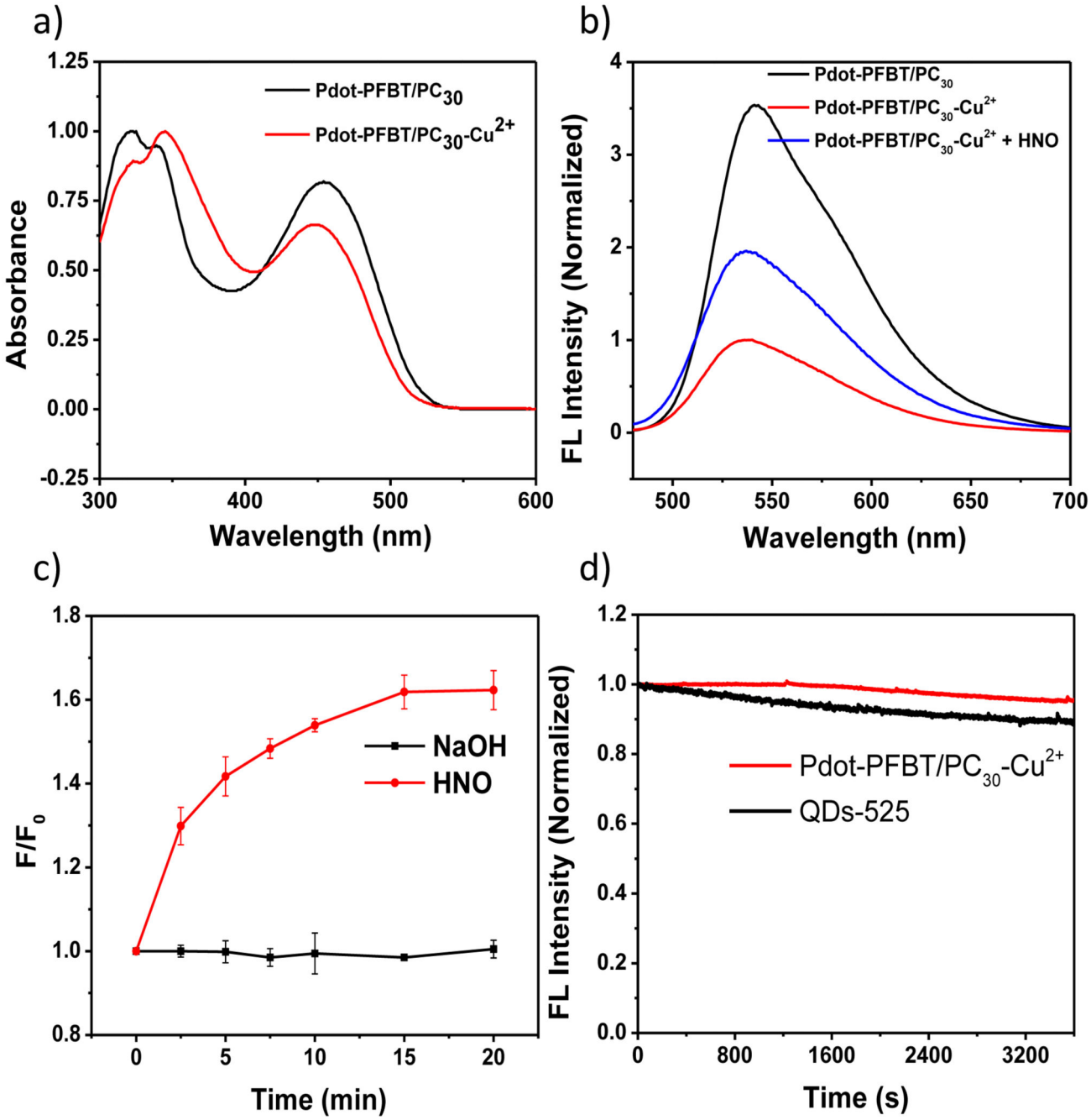

Fig. 2.

(a) UV absorption spectra and (b) fluorescence emission spectra (λ_{ex} = 450nm) of 1 ppm Pdot-PFBT/PC_{30} and Pdot-PFBT/PC_{30}-Cu^{2+} in PBS solution. (c) Time course experiment of Pdot-PFBT/PC_{30}-Cu^{2+} reacting with AS (400 μM) and NaOH (0.1 mM) in PBS solution (10 mM, pH 7.4). (d) Photostabilility of Pdot-PFBT/PC_{30}-Cu^{2+} and QDs-525 in PBS solution.

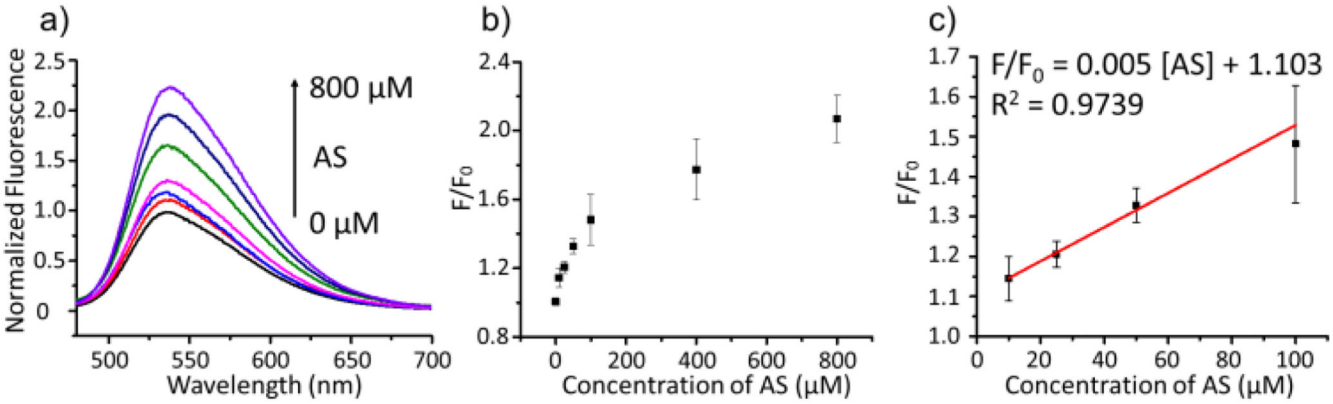

Fig. 3.

(a) Fluorescence spectra of Pdot-PFBT/PC_{30}-Cu^{2+} (1 ppm) in the presence of various concentrations of AS. λ_{ex} = 450 nm, λ_{em} = 450 nm – 700 nm. (b - c) Relationship between the relative fluorescence intensity at 537 nm and concentrations of AS (0, 10, 25, 50, 100, 400, and 800 μM). Fluorescence spectra were obtained in 10 mM PBS solution (pH = 7.4) after incubation for 20 min at 37 °C. λ_{ex} = 450 nm.

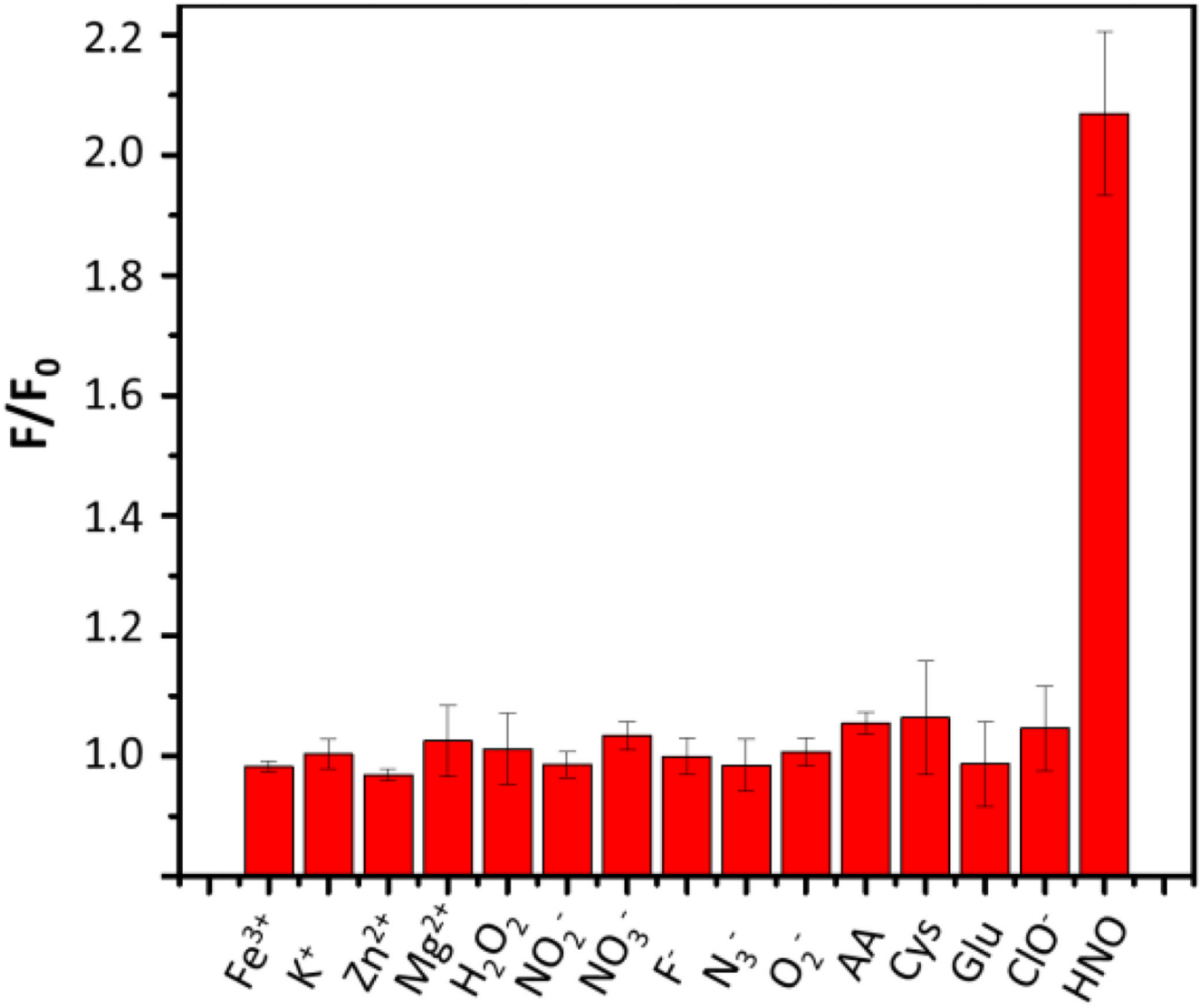

Fig. 4.

The fluorescence responses of the Pdot-PFBT/PC_{30}-Cu^{2+} (1 ppm) to various relevant redox species (1 mM) and 800 μM AS, in pH 7.4, 10 mM PBS solution.

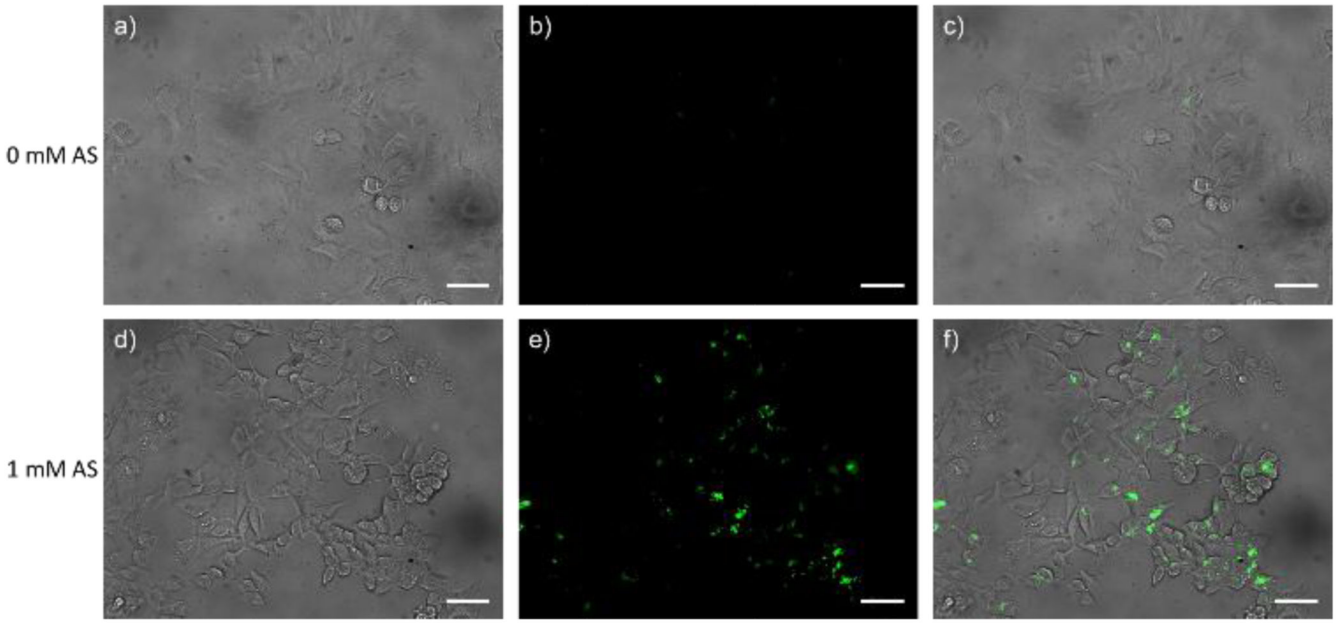

Fig. 5.

Fluorescence images of live MCF-7 cells. (a) bright-field image of living MCF-7 cells incubated with only Pdot-PFBT/PC_{30}-Cu^{2+}; (b) fluorescence image of (a); (c) merged image of (a) and (b). (d) bright-field image of living MCF-7 cells incubated with Pdot-PFBT/PC_{30}-Cu^{2+} and 1 mM AS; (e) fluorescence image of (d); (f) merged image of (d) and (e). The scale bar is 50 μm.

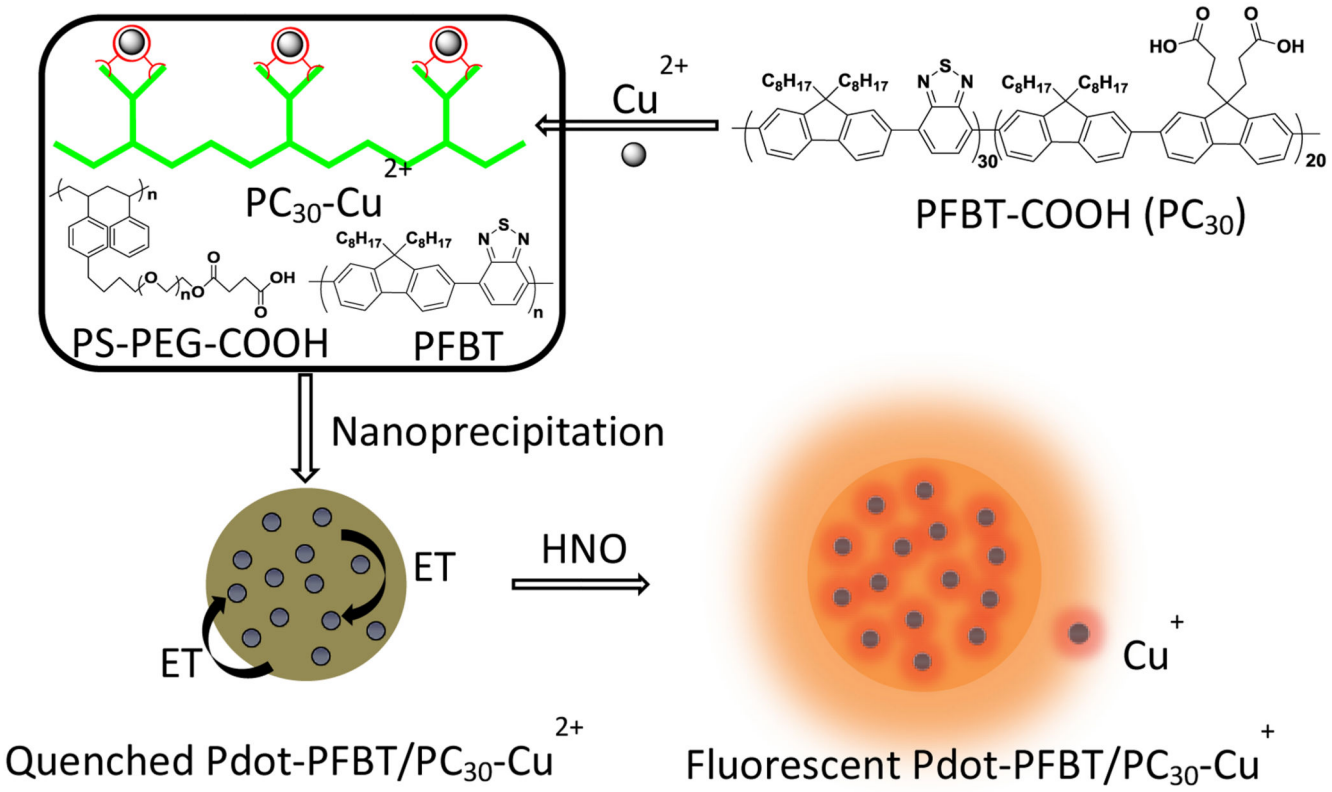

Scheme 1.

Schematic showing the fabrication of the Pdot-PFBT/PC_{30}-Cu^{2+} Pdots for the detection of nitroxyl (HNO). The fluorescence of Pdots was quenched by Cu^{2+} through electron transfer. When Cu^{2+} was reduced to Cu^{+} in the presence of HNO, it restored the fluorescence of Pdots.